



7N-02
197173
158

TECHNICAL NOTE

D-157

EXPERIMENTAL PRESSURE DISTRIBUTIONS OVER
BLUNT TWO- AND THREE-DIMENSIONAL BODIES HAVING SIMILAR
CROSS SECTIONS AT A MACH NUMBER OF 4.95

By Jerome D. Julius

Langley Research Center
Langley Field, Va.

NATIONAL AERONAUTICS AND SPACE ADMINISTRATION
WASHINGTON

September 1959

(NASA-TN-D-157) EXPERIMENTAL PRESSURE
DISTRIBUTIONS OVER BLUNT TWO- AND
THREE-DIMENSIONAL BODIES HAVING SIMILAR
CROSS SECTIONS AT A MACH NUMBER OF 4.95
(NASA. Langley Research Center) 15 p

N89-71291

Unclas
00/02 0197173

A

NATIONAL AERONAUTICS AND SPACE ADMINISTRATION

TECHNICAL NOTE D-157

EXPERIMENTAL PRESSURE DISTRIBUTIONS OVER
BLUNT TWO- AND THREE-DIMENSIONAL BODIES HAVING SIMILAR
CROSS SECTIONS AT A MACH NUMBER OF 4.95

By Jerome D. Julius

SUMMARY

L
4
5
8

Measurements of the pressure distribution about two- and three-dimensional bodies having flat, hemispherical, and oval leading edges (nose shapes) have been made at a Mach number of 4.95 and at Reynolds numbers per foot ranging from 15×10^6 to 75×10^6 . The results were compared with modified Newtonian theory with and without any consideration of the centrifugal forces present in the flow field.

INTRODUCTION

In order to reduce the heat-transfer rate at the forward portion of bodies traveling at supersonic and hypersonic velocities, it is necessary to blunt the leading edges and nose shapes. Blunting will change the aerodynamic characteristics of the body. Of great importance is the effect on the pressure distribution, for it is essential to the study of many of the aerodynamic characteristics of the body. Consequently, a program has been undertaken in the Langley Gas Dynamics Branch to study the pressure distributions and heat-transfer rates about blunt bodies. (For example, see refs. 1 and 2.) The purpose of this paper is to present experimental pressure-distribution data obtained for two- and three-dimensional bodies having similar cross sections.

SYMBOLS

C_p	local pressure coefficient, $\frac{p_l - p_\infty}{\frac{\gamma}{2} p_\infty M_\infty^2}$
$C_{p,max}$	maximum pressure coefficient, $\frac{p_{t,l} - p_\infty}{\frac{\gamma}{2} p_\infty M_\infty^2}$
M	Mach number
p	pressure, lb/sq in.
r	base radius of bodies of revolution, in.
$R_{D,\infty}$	free-stream Reynolds number based on maximum base diameter of three-dimensional models
$R_{T,\infty}$	free-stream Reynolds number based on maximum body thickness of two-dimensional models
s	distance along body surface measured from stagnation point, in.
t	one-half maximum body thickness of two-dimensional models, in.
x	distance parallel to axis of symmetry measured from stagnation point, in.
y	distance from axis of symmetry to outer surface of model, in.
γ	ratio of specific heats
Subscripts:	
l	conditions just behind a normal shock
l	local conditions
max	maximum
t	stagnation conditions
∞	free-stream conditions

APPARATUS AND TESTING PROCEDURE

Tests of two- and three-dimensional bodies having flat, hemispherical, and oval leading edges were conducted at a Mach number of 4.95 in a 9-inch blowdown, axial-symmetric jet in the Langley gas dynamics laboratory at a stagnation temperature of approximately 860° R for Reynolds numbers per foot ranging from 15×10^6 to 75×10^6 . The pressure measurements were made with 16-inch-dial test gages or a 10-foot mercury manometer, or both. The mercury manometer was used to measure the lower pressures and the gages were used to measure the higher pressures. The gages were selected to give the greatest gage-reading accuracy possible for the measurement in question.

Figure 1(a) shows the two-dimensional model installed in the tunnel test section in testing position. The pressures were measured in a plane parallel to the flow at the midspan. Two additional measuring stations for the stagnation pressure were located 1.5 inches on each side of the midspan. The data from these two stations were used to check for any three-dimensional effects. Because of difficulties encountered in establishing supersonic flow in the tunnel with the model initially in the test section, the tunnel was brought to steady operating conditions (supersonic conditions) and the model was then injected into the flow by means of a pneumatic actuator. Data were recorded after uniform flow (supersonic flow) was reestablished. Reestablishment of supersonic flow was checked by noting the tunnel static pressure before and after the injection of the model in the test section of the tunnel. Figure 1(b) shows the installation for testing the three-dimensional models. The shaded areas shown in figure 1(b) are cross-sectional views of the support.

Model geometry is shown in figure 2. The two-dimensional models have a 7-inch span, and end plates are mounted on them in order to reduce any three-dimensional effects. The contours of the oval models were determined by a prescribed pressure distribution. (See ref. 1, body $C_4 = 0.586$.) The models were fabricated from type 416 stainless steel.

RESULTS

The experimental results are expressed as the ratio of the local pressure coefficient of the model to the stagnation (maximum) pressure coefficient of the model, and this ratio is plotted against the distance from the stagnation point divided by one-half the maximum thickness of the model.

The experimental pressure distributions for the two- and three-dimensional models with flat leading edges are shown in figures 3(a) and 3(b) along with the result of modified Newtonian theory (ref. 3). The theory in this case fails to predict any pressure variation across the face of the body. The pressures decrease at a lower rate over the three-dimensional model than over the two-dimensional model.

The experimental pressure distributions for the oval two- and three-dimensional models are shown in figures 3(c) and 3(d), along with the results of modified Newtonian theory with and without centrifugal-force corrections. The pressures over these two models decrease at approximately the same rate.

The experimental pressure distributions for the hemispherical two- and three-dimensional models are shown in figures 3(e) and 3(f), along with the result of modified Newtonian theory with and without centrifugal-force corrections. The pressures decrease at a faster rate over the three-dimensional model than over the two-dimensional model. The difference in agreement with modified Newtonian flow between the two- and three-dimensional models is perhaps related to the flow picture explained in reference 4. In reference 4, it is pointed out that there is an increase in pressure just behind the shock as compared with the pressure behind a concentric shock. This increase in pressure is opposed by a reduction in pressure across the shock layer due to reduced centrifugal forces. The centrifugal forces are reduced because the radii of curvature of the streamlines increase with distance normal to the body surface. The resulting net pressure for the three-dimensional body is very close to that predicted by the modified Newtonian theory, which neglects the increase in pressure behind the shock due to shock divergence from the body as well as the reduction in pressure across the shock layer due to reduced centrifugal forces. It appears that the two opposite effects are of the same magnitude and cancel for this case. For the two-dimensional model it appears that the shock divergence effect predominates and hence a higher net pressure results. The preceding discussion is restricted to the hemispherical models inasmuch as it can be seen from figures 3(a) and 3(b) that the shock divergence effect seems to be reversed for the flat-face models.

Figures 4(a) and 4(b) show that for the hemispherical two- and three-dimensional models, the present data are in agreement with existing data (refs. 2 and 5 to 10). Existing data cover a Mach number range of 1.98 to 18.80 and a free-stream Reynolds number range based on maximum body thickness of 6.7×10^3 to 6.7×10^6 . The tests of reference 8 were the only tests conducted in a helium tunnel.

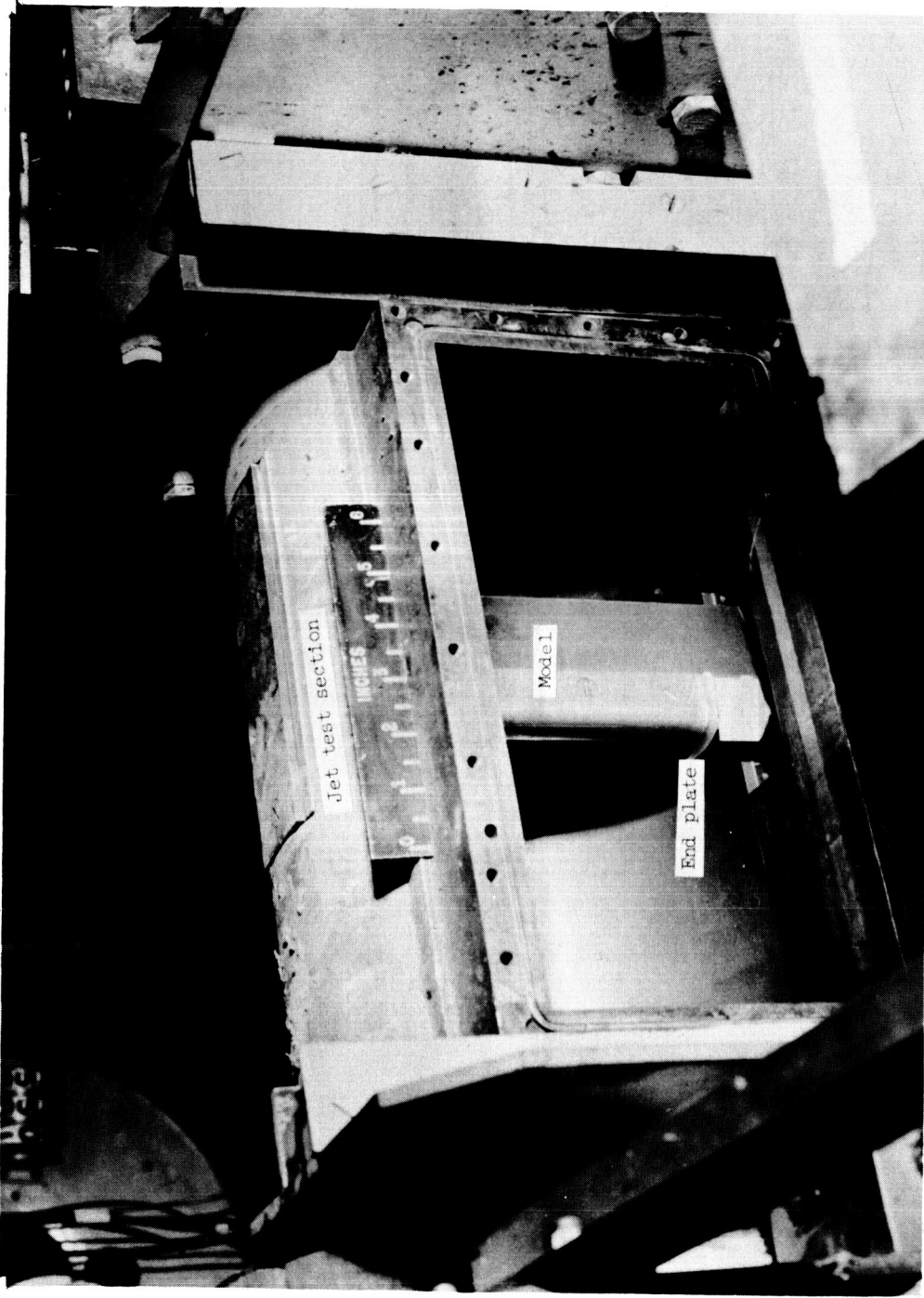
CONCLUDING REMARKS

Measurements of the pressure distributions about two- and three-dimensional bodies having flat, hemispherical, and oval leading edges have been made at a Mach number of 4.95 and at Reynolds numbers per foot ranging from 15×10^6 to 75×10^6 . For the hemispherical models, the pressures decreased faster with distance from the stagnation point over the three-dimensional model than over the two-dimensional model. For the flat-leading-edge models, the reverse was true. The pressures over the oval-leading-edge models decreased at approximately the same rate. Modified Newtonian theory, without centrifugal-force corrections, predicted pressures on the hemispherical three-dimensional model very well.

Langley Research Center,
National Aeronautics and Space Administration,
Langley Field, Va., June 1, 1959.

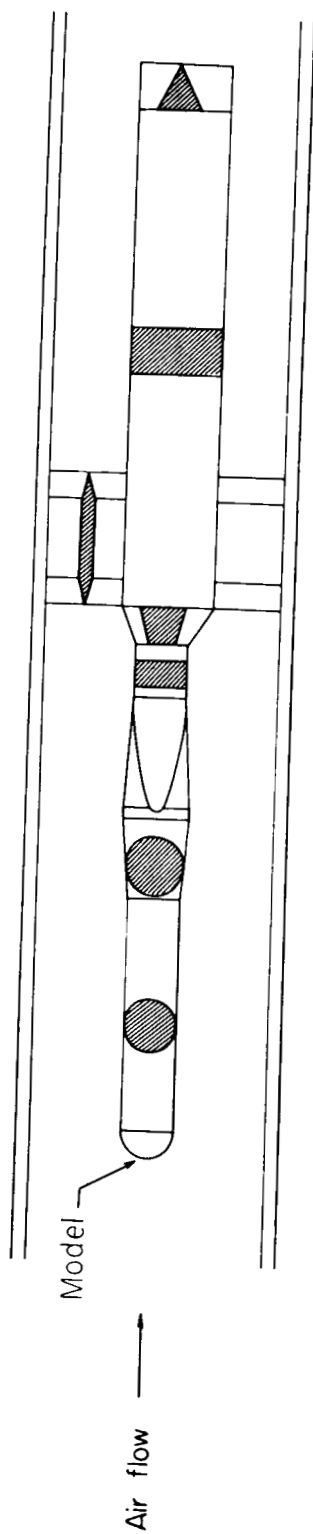
REFERENCES

1. Cooper, Morton, and Mayo, Edward E.: Measurements of Local Heat Transfer and Pressure on Six 2-Inch-Diameter Blunt Bodies at a Mach Number of 4.95 and at Reynolds Numbers Per Foot Up to 81×10^6 . NASA MEMO 1-3-59L, 1959.
2. Beckwith, Ivan E., and Gallagher, James J.: Heat Transfer and Recovery Temperatures on a Sphere With Laminar, Transitional, and Turbulent Boundary Layers at Mach Numbers of 2.00 and 4.15. NACA TN 4125, 1957.
3. Ivey, H. Reese, Klunker, E. Bernard, and Bowen, Edward N.: A Method for Determining the Aerodynamic Characteristics of Two- and Three-Dimensional Shapes at Hypersonic Speeds. NACA TN 1613, 1948.
4. Lees, Lester: Recent Developments in Hypersonic Flow. Jet Propulsion, vol. 27, no. 11, Nov. 1957, pp. 1162-1178.
5. Oliver, Robert E.: An Experimental Investigation of Flow Over Simple Blunt Bodies at a Nominal Mach Number of 5.8. GALCIT Memo. No. 26 (Contract No. DA-04-495-Ord-19), June 1, 1955.
6. Goodwin, Glen, Creager, Marcus O., and Winkler, Ernest L.: Investigation of Local Heat-Transfer and Pressure Drag Characteristics of a Yawed Circular Cylinder at Supersonic Speeds. NACA RM A55H31, 1956.
7. Crawford, Davis H., and McCauley, William D.: Investigation of the Laminar Aerodynamic Heat-Transfer Characteristics of a Hemisphere-Cylinder in the Langley 11-Inch Hypersonic Tunnel at a Mach Number of 6.8. NACA Rep. 1323, 1957. (Supersedes NACA TN 3706.)
8. Vas, I. E., Bogdonoff, S. M., and Hammitt, A. G.: An Experimental Investigation of the Flow Over Simple Two-Dimensional and Axial Symmetric Bodies at Hypersonic Speeds. Rep. No. 382 (WADC TN 57-246), Dept. Aero. Eng., Princeton Univ., June 1957.
9. Gowen, Forrest E., and Perkins, Edward W.: Drag of Circular Cylinders for a Wide Range of Reynolds Numbers and Mach Numbers. NACA TN 2960, 1953.
10. Chauvin, Leo T.: Pressure Distribution and Pressure Drag for a Hemispherical Nose at Mach Numbers 2.05, 2.54, and 3.04. NACA RM L52K06, 1952.



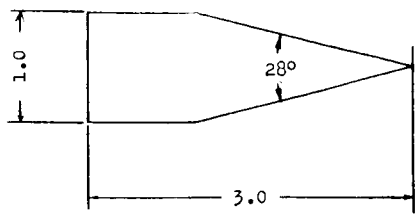
(a) Installation for two-dimensional model. L-58-67a.1

Figure 1.- Model installation.

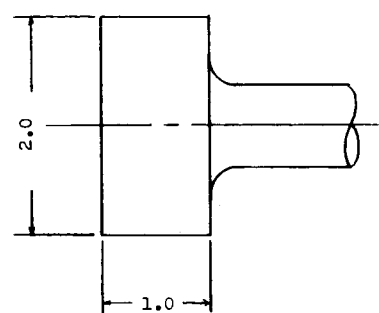


(b) Fixed-support installation for three-dimensional models.

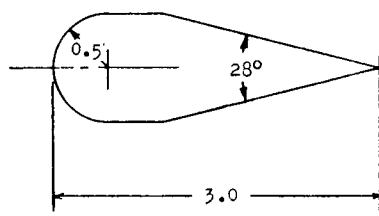
Figure 1.- Concluded.



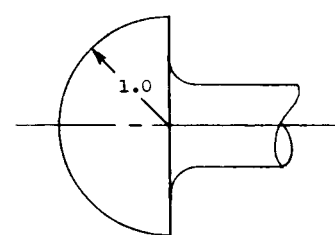
(a) Flat, two-dimensional model.



(b) Flat, three-dimensional model.



(c) Hemisphere, two-dimensional model.

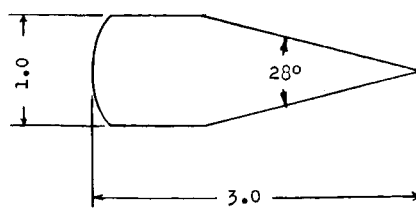


(d) Hemisphere, three-dimensional model.

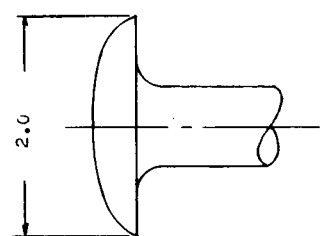
Dimensionless contour coordinates
for oval models

$$[y_{\max} = \frac{1}{2} \text{ max. model thickness}]$$

$\frac{x}{y_{\max}}$	$\frac{y}{y_{\max}}$
0	0
.019	.417
.038	.524
.057	.598
.076	.656
.095	.703
.113	.744
.132	.779
.151	.810
.170	.838
.189	.863
.208	.885
.227	.905
.246	.922
.265	.938
.284	.952
.303	.965
.321	.976
.340	.985
.359	.993
.378	1.000

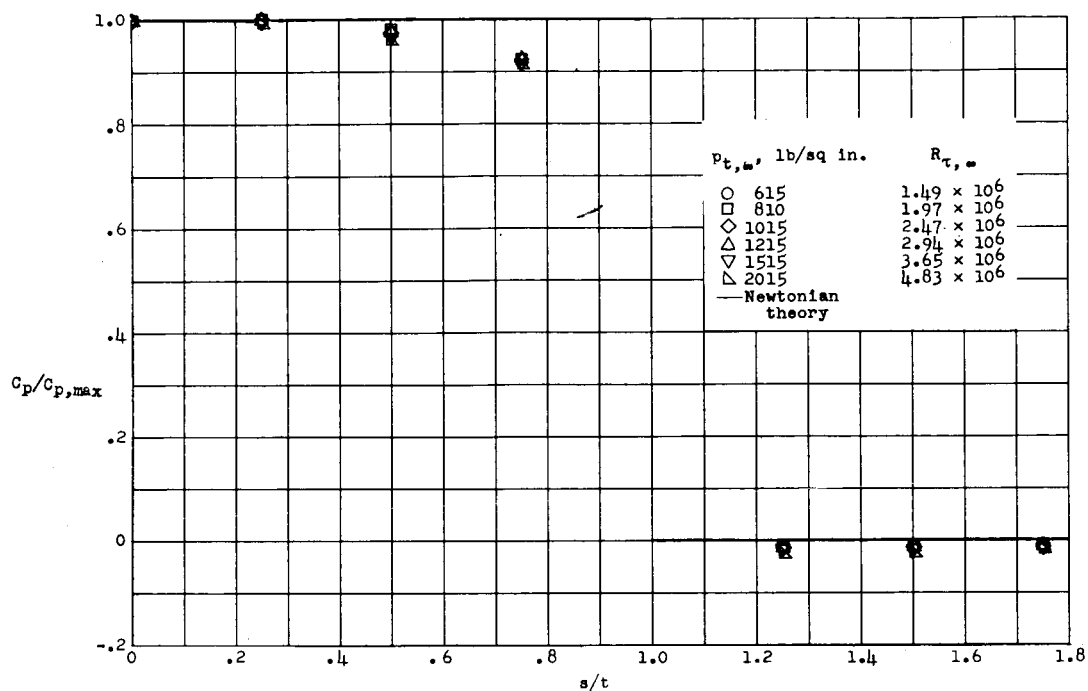


(e) Oval, two-dimensional model.

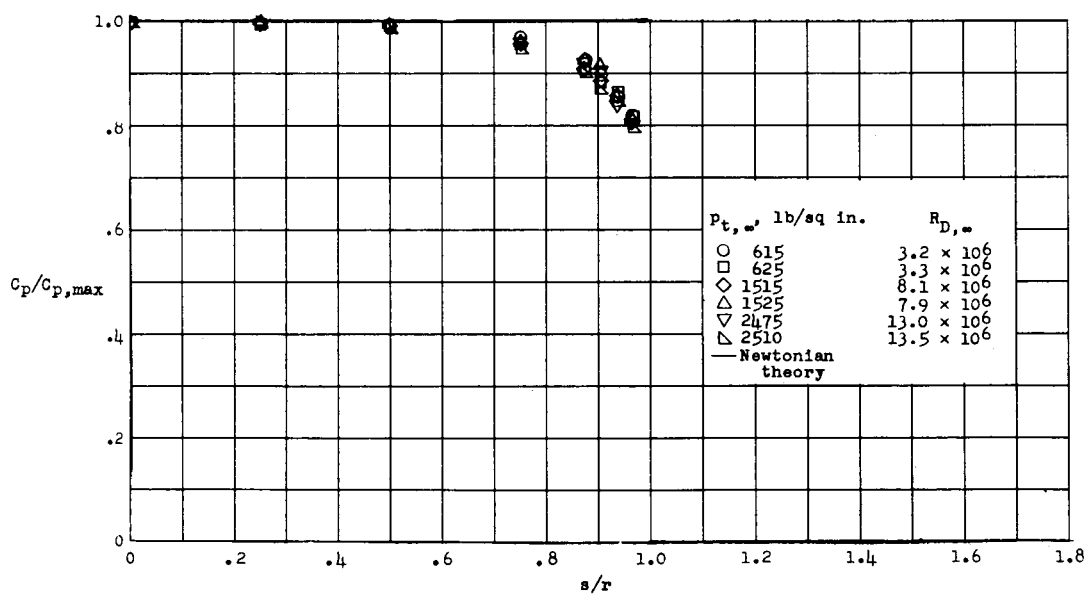


(f) Oval, three-dimensional model.

Figure 2.- Model geometry. (All dimensions are in inches.)

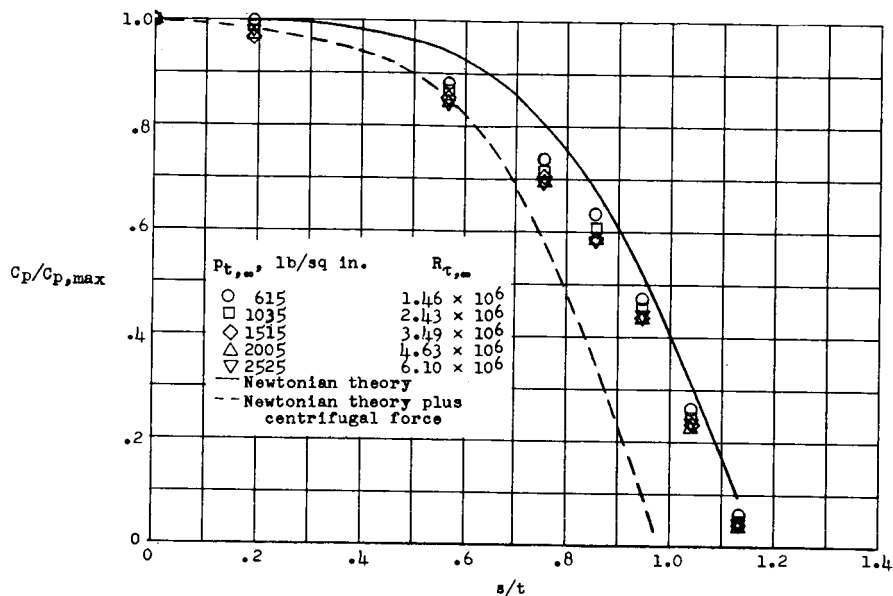


(a) Flat, two-dimensional model.

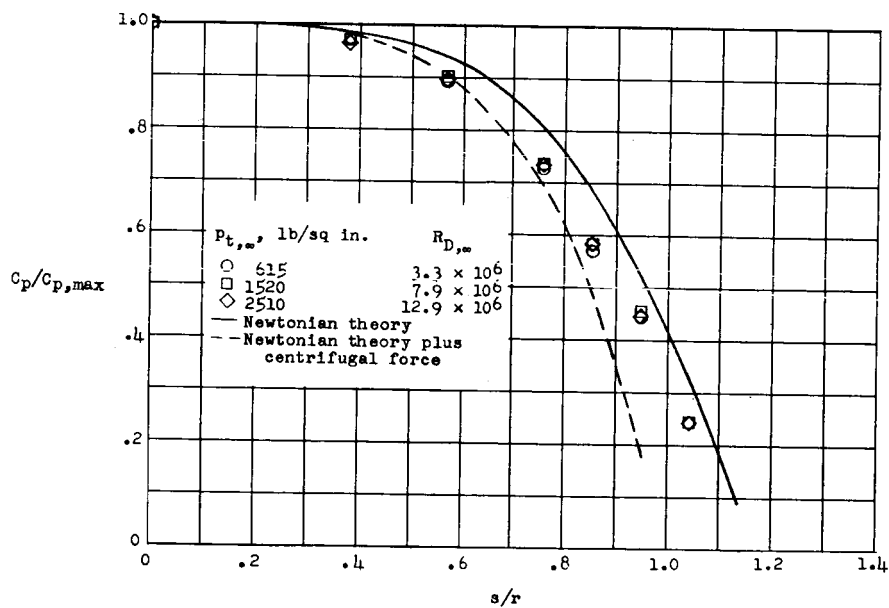


(b) Flat, three-dimensional model.

Figure 3.- Comparison of experimental and theoretical pressure distribution for $M = 4.95$.

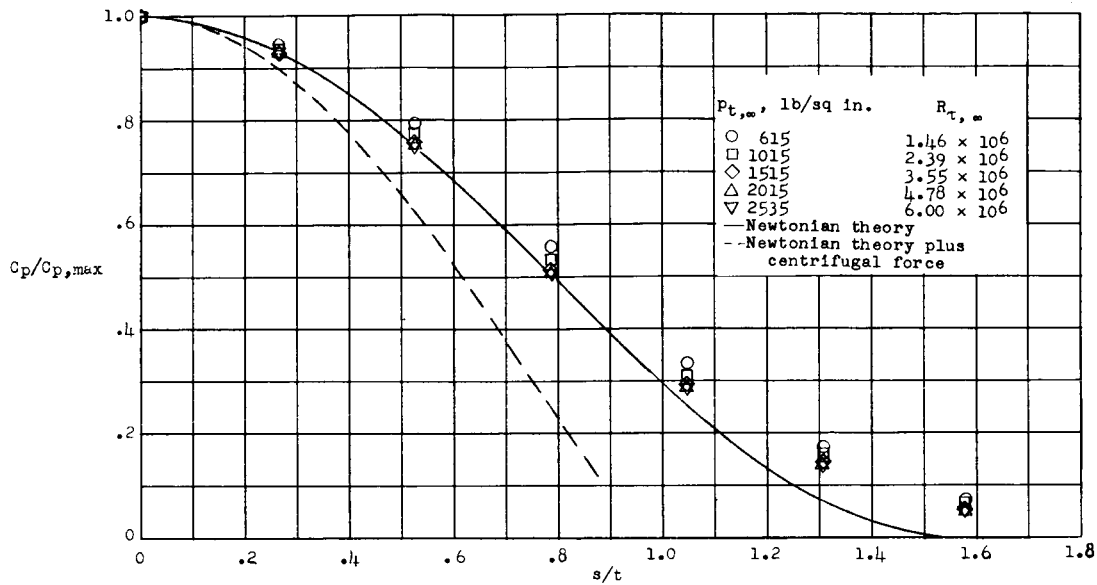


(c) Oval, two-dimensional model.

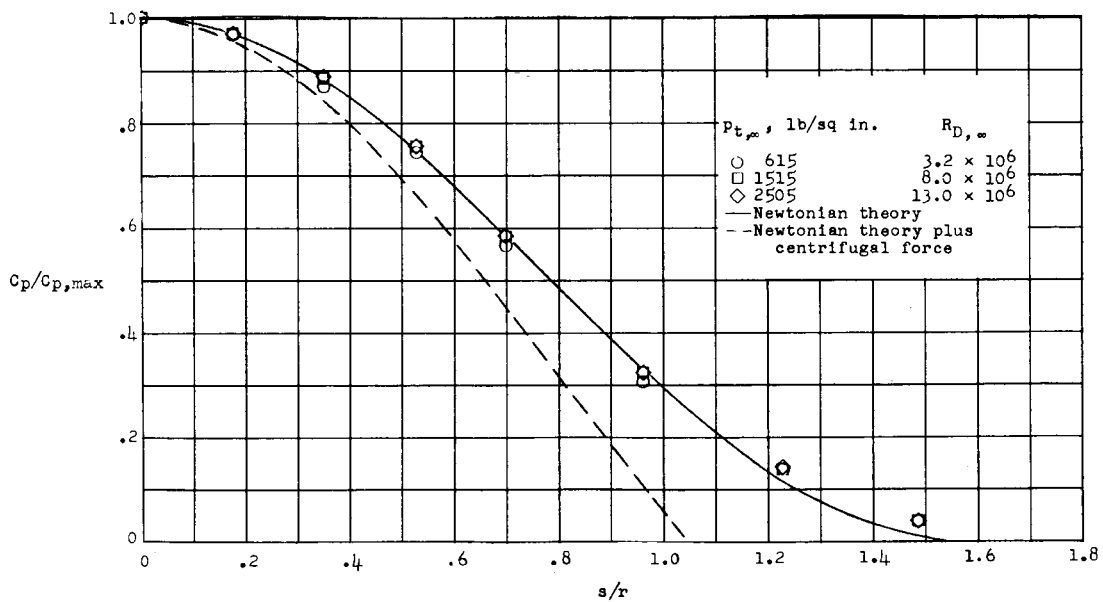


(d) Oval, three-dimensional model.

Figure 3.- Continued.

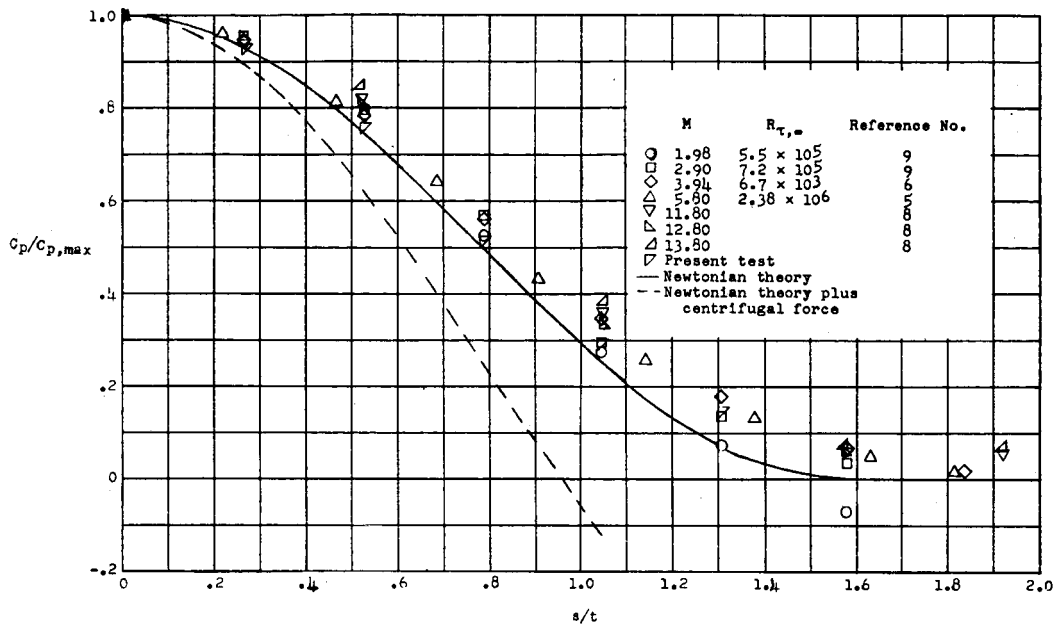


(e) Hemisphere, two-dimensional model.

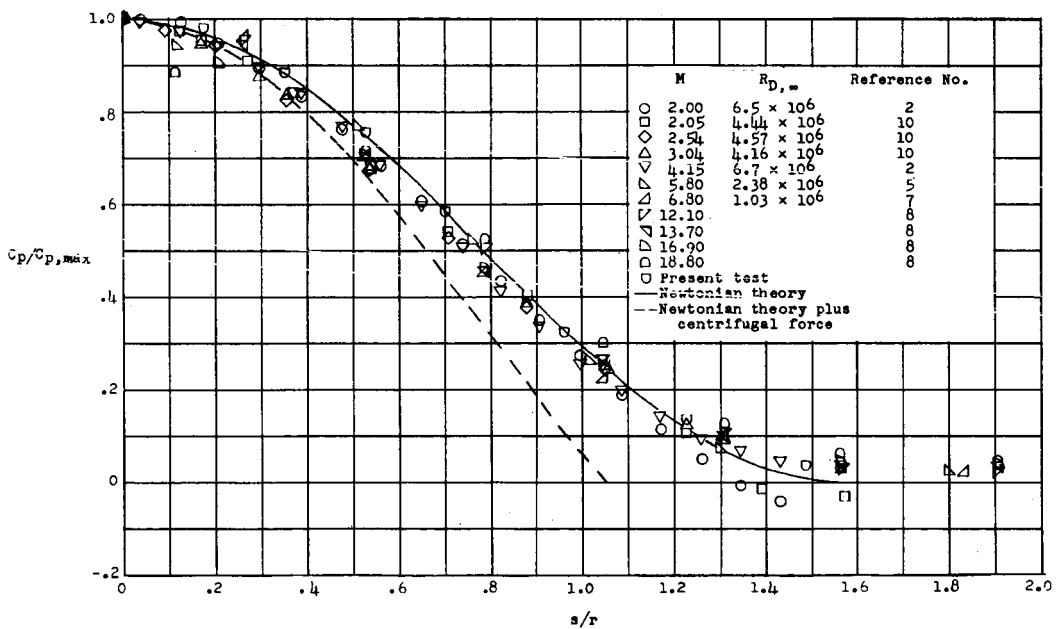


(f) Hemisphere, three-dimensional model.

Figure 3.- Concluded.



(a) Hemisphere, two-dimensional models.



(b) Hemisphere, three-dimensional models.

Figure 4.- Comparison of present data with existing data for hemispherical models.